

Electronic, superconducting, and optical properties of technetium from its augmented-plane-wave band structure

Parsathi Chatterjee

Department of General Physics and X-rays, Indian Association for the Cultivation of Science, Jadaupur, Calcutta 700 032, India

(Received 14 May 1982; revised manuscript received 27 August 1982)

The detailed energy-band structure of hexagonal-close-packed technetium, corresponding to the atomic configuration $4d^5 5s^2$ of its seven outermost valence electrons, has been obtained throughout the Brillouin zone using the composite-wave variational version of the augmented-plane-wave (APW) method in conjunction with the $X\alpha$ ($\alpha=0.70299$) exchange approximation for obtaining the potentials. From the band-structure data the electronic density of states (DOS) and the angular-momentum-decomposed DOS were calculated by the accurate Gilat-Raubenheimer method. These quantities were used to calculate the electron-phonon coupling constant and the transition temperature (T_c) using the theories of Gaspari and Gyorffy and of McMillan. Also studied were the Fermi surface and the optical properties of Tc via the imaginary part of the interband dielectric constant for bound electrons, the latter being the first of such a study on Tc to date. The superconducting properties and the Fermi surface which could be compared to experiments show, in general, satisfactory agreement.

I. INTRODUCTION

Technetium is an interesting metal in that, although its atomic number is only 43, all its isotopes are radioactive, with the longest-lived ^{99}Tc decaying with a half-life of 2.1×10^5 yr. Recent experiments on Tc have revealed yet another interesting property. Its superconducting transition temperature (T_c), which has been raised up to 11.2 K (Ref. 1), has surpassed even that of Nb. If one assumes that it is the electron-phonon interactions which give rise to pairing between electrons, then T_c should depend chiefly on the electron-phonon coupling constant, or mass enhancement factor λ . Since much progress^{2,3} has recently been made to predict λ (and thence⁴ T_c) from energy-band data, it would be interesting to calculate these quantities from the energy-band structure of Tc. Two such approximate calculations of T_c exist. In the first case Papaconstantopoulos *et al.*,³ in the process of their extensive study of T_c of elements with $Z \leq 49$, obtained the superconducting properties of technetium after assigning an fcc structure to the material. Their calculated value of 0.03 K for T_c is far away from the measured range of 4.6–11.2 K,¹ and the authors assigned this difference to the incorrect structure assumed for the solid. With this in mind, Asokamani and Iyakutti⁵ have recently calculated the transition temperature from the energy-band data taking into account the actual

crystal structure. However, although they have obtained rather good agreement with experiments, the defect in their calculations lies in the arbitrary assumption of equating the angular-momentum-decomposed component density of states (DOS) to the corresponding free-electron value for $l \neq 2$, which in view of some recent calculations on transition elements,^{3,6} and the present results appear unjustified. Since the theory of Gaspari and Gyorffy (GG), which has already proved very reliable in predicting the T_c of cubic elements,^{2,3,6} compounds,^{7,8} and alloys,^{9,10} is yet to be properly tested for the hcp structure, we feel that an attempt in this direction could be made by conducting an extensive study of the energy bands of Tc throughout its hcp Brillouin zone (BZ) and predicting λ according to the unapproximated GG formula.

The electronic energy-band structure of solids is an accurate tool for predicting other material properties as well. Thus one may predict the optical properties in the form of the imaginary part of the interband dielectric constant for bound electrons ϵ_2^b as a function of the excitation frequency ω .¹¹ No effort, theoretical or practical, has yet been made to predict such properties for Tc. However, in view of experiments by Weaver, Lynch, and Olson,¹² we feel that such a study for Tc would not only be most relevant and stimulating to experimentalists, but would also serve to identify the location in \vec{k} space

of the important optical excitations in the metal. Furthermore, in metals it is necessary to have accurate predictions of Fermi surfaces in order to calculate such properties as superconductivity and the phonon spectra. Only two previous calculations of the Fermi surface of Tc exist to date,^{5,13} both of which have utilized the Korringa-Kohn-Rostoker (KKR) method. Since the Fermi surface of the metal has not yet been calculated from augmented-plane-wave (APW) energy-band data, it would be interesting to make a comparative study of the Fermi surfaces obtained from the two leading methods of band-structure study, in light of the de Haas-van Alphen results¹⁴ for Tc.

With these goals in mind, we present here an accurate study of the energy-band structure of hcp Tc by the composite-wave variational version¹⁵ of the APW method in conjunction with the $X\alpha$ exchange approximation for obtaining the potentials. Also presented are the DOS, the Fermi surface, and the superconducting and the optical properties of the metal as calculated from these energy-band data.

III. OUTLINE OF THE METHOD

The crystal potential of the muffin-tin (MT) type was generated by a method¹⁶ in which the spherically symmetric contributions from 14 sets of nearest neighbors are superposed on the potential of the central atom. The atomic charge densities used in constructing the MT potentials were the results of a modified Hartree-Fock-Slater self-consistent-field program,¹⁷ wherein the exchange contribution was calculated via the $X\alpha$ exchange approximation, using $\alpha=0.70299$ for Tc.¹⁸ The configuration assumed for obtaining the charge densities is $4d^55s^2$. The MT zero was taken at the potential obtained by performing a spherical average of the potential in the interstitial region between the APW spheres and the Wigner-Seitz sphere. The lattice constants used were $a=5.17958$ a.u. and $c=8.29868$ a.u.¹⁹ The MT radius was taken at 2.4596 a.u.

With the help of these potentials the electronic energy-band structure was obtained using the composite-wave variational version¹⁵ of the APW method. Simultaneously, the s , p , d , and f components of the fractional-charge densities inside the APW spheres were calculated by the method described by Mattheiss, Wood, and Switendick.²⁰ A total of 126 points in the irreducible $\frac{1}{24}$ th wedge of the BZ (including all the symmetry points and directions) were studied thus from first principles. These results were then interpolated to a finer mesh of 24×4200 \vec{k} points in the BZ via the Lagrangian interpolation scheme in order to obtain the Fermi energy E_F , the DOS $m(E)$, and its angular-momentum

components $m_l(E)$, inside the APW spheres. In order to calculate $m(E)$ and $m_l(E)$, we have made use of the Raubenheimer-Gilat formula^{21,22}

$$m(E) = \sum_n \sum_{\vec{k}_0} W_{\vec{k}_0} \frac{\Delta S(n, E, \vec{k}_0)}{|\vec{\nabla}_{\vec{k}} E_n(\vec{k}_0)|} \quad (1)$$

and its modification⁷

$$m_l(E) = \sum_n \sum_{\vec{k}_0} W_{\vec{k}_0} \frac{Q_{n,l}(\vec{k}_0) \Delta S(n, E, \vec{k}_0)}{|\vec{\nabla}_{\vec{k}} E_n(\vec{k}_0)|} \quad (2)$$

Here ΔS is the element of the energy surface intercepted within the cube centered at \vec{k}_0 , $Q_{n,l}(\vec{k}_0)$ is the fractional-charge density inside the APW spheres,²⁰ n is the band index, and $W_{\vec{k}_0}$ is a weight factor associated with the symmetry of \vec{k}_0 . The values of these quantities at E_F are required to calculate the electron-phonon coupling constant and the superconducting transition temperature in the manner described below.

In the rigid-ion strong-coupling theory, λ is given by⁴

$$\lambda = \frac{\eta}{M \langle \omega^2 \rangle} \quad (3)$$

where η may be calculated using the following formula due to Gaspari and Gyorffy²:

$$\begin{aligned} \eta &= m(E_F) \langle I^2 \rangle \\ &= \frac{2E_F}{\pi^2 m(E_F)} \sum_l (l+1) \sin^2(\delta_l - \delta_{l+1}) \\ &\quad \times \frac{m_l(E_F) m_{l+1}(E_F)}{m_l^{(1)}(E_F) m_{l+1}^{(1)}(E_F)} \quad (4) \end{aligned}$$

Here $\langle \omega^2 \rangle$ is an average of the square of the phonon frequency,⁴ M is the atomic mass, δ_l is the phase shift of the l th partial wave due to the MT potential evaluated at E_F , and $m(E_F)$, $m_l(E_F)$, and $m_l^{(1)}(E_F)$ are the total, component, and the "single-scatterer" component DOS,⁶ respectively, at E_F . To obtain this formula GG expanded² the square of the electron-phonon matrix element averaged over the Fermi surface, $\langle I^2 \rangle$, in terms of Bloch functions:

$$\Psi_{\vec{k}}(\vec{r}) = \sum_l \sum_{m=-l}^l a_{l,m}(\vec{k}) R_l(r, E_{\vec{k}}) Y_l^m(\hat{r}) \quad (5)$$

where $Y_l^m(\hat{r})$ is a spherical harmonic and $R_l(r, E_{\vec{k}})$ is the asymptotic solution of the radial Schrödinger equation. In this equation the effect of the ion at the origin is mainly included in $R_l(r, E_{\vec{k}})$ and considered exactly, while the coefficient, $a_{l,m}(\vec{k})$, that is determined by the crystal structure, is approximated

by

$$a_{l,m}(\vec{k}) = a_l(E_{\vec{k}}) Y_l^m(\hat{k}). \quad (6)$$

This is a drastic approximation for it assumes that the bands are spherical. However, John²³ has shown, by expanding $\langle I^2 \rangle$ in terms of the retarded Green's function, that in cubic crystals for $l \leq 2$ this approximation is completely unnecessary and that a rigorous evaluation gives exactly the same formula for η . This is only to be expected since the cubic harmonics are the same as the spherical harmonics to this order of l .²⁴ However, for f and higher-order scattering in cubic crystals (it may be noted that d - f scattering provides an appreciable contribution to η in transition metals³) and for crystals of lower symmetry, this approximation becomes necessary. In terms of the multiple-scattering theory, this means neglecting the nondiagonal elements of the imaginary part of the scattering path operator, T_{LL}^{ii} ,²³ although in the spherical approximation the diagonal elements of $\text{Im}T_{LL}^{ii}$ are replaced by an average which depends upon the angular momentum. In defense, therefore, for the application of Eq. (4) to hcp Tc, which is what we propose to do, it may be pointed out, as with GG,² that, as this approximation retains most of the nonstructural features of the real energy-band structure, it is likely to give a fair idea of η and thence the superconducting properties of the metal.

To come back to Eq. (4), E_F , $m(E_F)$, and $m_l(E_F)$ may be calculated from the energy-band data while the usual expressions for δ_l and $m_l^{(1)}(E_F)$ are given in, e.g., Ref. 9. Thus having obtained all the quantities in Eqs. (3) and (4), T_c can be obtained from the usual McMillan formula⁴:

$$T_c = \frac{\Theta_D}{1.45} \exp \left[\frac{-1.04(1+\lambda)}{\lambda - \mu^*(1+0.62\lambda)} \right], \quad (7)$$

where Θ_D is the Debye temperature and μ^* is the Coulomb pseudopotential which may be taken as 0.13 for a transition element.⁶

In order to calculate the optical properties, we have made use of the photon energy distribution function $D(\omega)$, for the total number of allowed transitions between the occupied and the unoccupied parts of various bands for photon energies between ω and $\omega + \Delta\omega$. This is given by

$$D(\omega) = \sum_{l \neq u} \int d^3k f(E_l(\vec{k})) \times [1 - f(E_u(\vec{k}))] |\langle u | \vec{p} | l \rangle|^2 \times \delta(E - E_u(\vec{k})) \delta(E - \omega - E_l(\vec{k})), \quad (8)$$

where f is the Fermi function, $\langle u | \vec{p} | l \rangle$ the momentum matrix element, and $E_u(\vec{k})$ and $E_l(\vec{k})$ the energies of an electron with wave vector \vec{k} in the upper energy band u and the lower energy band l , respectively. $D(\omega)$ is proportional to $\omega^2 \epsilon_2^b(\omega)$, where $\epsilon_2^b(\omega)$ is the imaginary part of the interband dielectric function for bound electrons.

The matrix elements in Eq. (8) are time consuming to include in a complete BZ integration. The approximation of constant matrix elements, which will be used in this paper, is believed to affect only the strength of the peaks.^{11,25} Although this is true for sharp peaks, fine structures like the shoulders and the splittings of the peaks may depend on the variation of the matrix elements with energy. However,

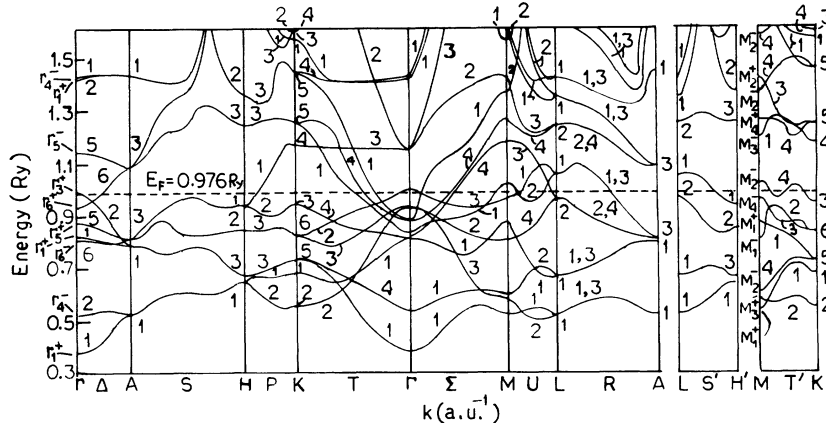


FIG. 1. Energy bands of Tc in the $X\alpha$ exchange approximation.

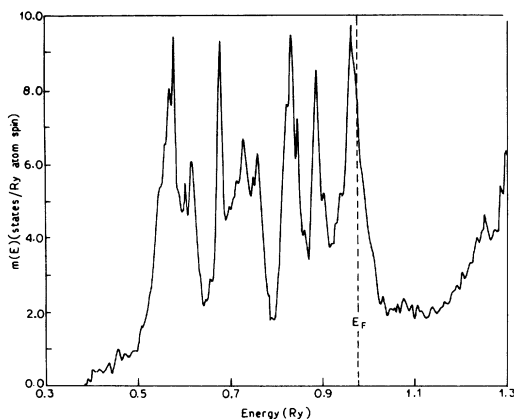


FIG. 2. Density of states of Tc. E_F denotes the Fermi energy.

to obtain a rough idea of the optical properties, it is sufficient to use this approximation, whereby, at 0 K, where our theoretical calculations are valid, $D(\omega)$ becomes a function of

$$\sum_{l \neq u} \int d^3k \delta(E - E_u(\vec{k})) \delta(E - \omega - E_l(\vec{k})),$$

which is known as the joint density of states (JDOS) for interband transitions.

III. RESULTS AND DISCUSSION

A. The energy-band structure, Fermi level, and the density of states

Figure 1 shows the calculated energies at different symmetry points and axes of the hcp BZ with the zero of the potential chosen at the MT potential. The only published band-structure calculations for Tc are due to Asokamani *et al.*,²⁶ wherein they have made use of the KKR method with three different types of potentials including (i) only the Slater exchange (V_S) and including both exchange and correlation by (ii) Overhauser's prescription (V_H) and by

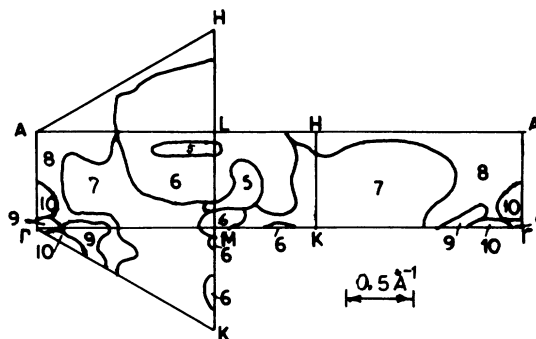


FIG. 3. Fermi-surface cross sections of Tc within the fundamental $\frac{1}{24}$ th wedge of the BZ. The numbers indicate the number of filled states below the Fermi level corresponding to the various regions of \vec{k} vectors.

(iii) the Vashishta-Singwi formalism (V_{VS}), respectively. The band diagram along the $\Gamma MK\Gamma$ direction is somewhat similar only to the one calculated using the potential V_H , although the number of bands crossing the Fermi level in our case is larger than theirs. Figure 1, however, bears a marked resemblance to the relativistic APW energy-band diagram (drawn with spin-orbit coupling neglected) for rhenium,²⁷ which lies just below Tc in the Periodic Table.

The Fermi energy E_F was computed from the energy-band data at 24×4200 \vec{k} points in the BZ such that the volume enclosed by the constant-energy surface is seven times the volume of the BZ. The value thus obtained is 0.976 Ry relative to the MT zero. The DOS was also calculated as previously described by the Raubenheimer-Gilat method²¹ and the resulting curve is shown in Fig. 2. Again the curve has some similarity to the one calculated by Asokamani and Iyakutti⁵ using V_H , but is more similar to the one obtained by Mattheiss for Re.²⁷ The value of the DOS at E_F , $m(E_F)$, as obtained by us, is 8.275 15 states/Ry atom spin. Table I compares our $m(E_F)$ value with all other calculations of

TABLE I. $m(E_F)$ (technetium), in units of states/Ry atom spin, for various calculations in the literature.

Potential with Hedin-Lundqvist exchange and correlation ³ (V_{HL})	Potential with Slater exchange ⁵ (V_S)	Potential with Overhauser exchange and correlation ⁵ (V_H)	Potential with Vashishta-Singwi exchange and correlation ⁵ (V_{VS})	Potential with $X\alpha$ exchange (present) ($V_{X\alpha}$)
7.86	9.452	7.616	8.398	8.275 15
fcc structure				

TABLE II. Phase shifts, component DOS, and single-scatterer component DOS.

	Phase shifts l of the potentials	l component of the DOS	Single-scatterer l component DOS
s	-1.080 13	0.156 08	0.202 03
p	-0.440 77	1.209 70	0.316 71
d	-1.164 64	4.902 85	5.145 50
f	0.012 33	0.172 34	0.060 80

this quantity in the literature. It may be observed that all the results, except the one using Slater exchange,⁵ lie quite close to each other, although the energy-band diagrams do not bear much similarity. In particular, it is surprising that, although the magnitude of the exchange and correlation terms suggests that the V_{VS} (Refs. 5 and 26) and the present $X\alpha$ exchange potentials should give very similar results for Tc, it is only in the value of $m(E_F)$ that this similarity is manifest—not in the energy-band diagram.

B. The Fermi surface

The Fermi-surface (FS) cross sections in the different planes of the $\frac{1}{24}$ th wedge of the BZ are shown in Fig. 3. The numbers represent the total of filled states below the various regions of \vec{k} vectors. The general features of the FS are similar to the KKR calculations of Faulkner¹³—although our figure contains some extra small pieces. Arko *et al.*¹⁴ have obtained the FS of Tc from de Haas—van Alphen measurements. Their observed frequencies seem to correspond to three hole surfaces around point L : two small pieces due to bands 5 and 6, which by group theory are degenerate if spin-orbit coupling effects are not considered, and a very large piece due to band 7. This is corroborated by the band-structure calculations of Asokamani and Iyakutti⁵ using the potentials V_H and V_{VS} and also by the relativistic energy-band data of Mattheiss for hcp Re.²⁷ However, the degenerate 5th and 6th bands in the present calculations lie close to, but do not cross, the Fermi level near point L , so that only one large

hole surface due to the 7th and 8th degenerate bands is obtained. This fact agrees with the FS calculations of Faulkner¹³ and of Asokamani and Iyakutti⁵ using the potential V_S . Another important observation from the de Haas—van Alphen experiments is the c branch of frequencies which is the only branch observed for all field angles. It has the shape of a lens and from the anisotropy of the surface should be located on the $A\Gamma$ line or at point H or K . Such a surface was not predicted by the FS calculations of Re.²⁷ However, a surface which is likely to correspond to this frequency in our figure is the one situated on the $A\Gamma$ line and having 10 filled states below it. In Faulkner's¹³ calculation, there is a similar surface at this position but having seven filled states below. The cross-section areas of this surface which intersect planes normal to the $[10\bar{1}0]$, $[11\bar{2}0]$, and $[0001]$ directions are found experimentally to be approximately 0.017, 0.018, and 0.032 a.u., respectively. In our case they are 0.0218, 0.017, and 0.022 a.u. as compared to 0.025, 0.0026, and 0.044 a.u. with potential V_I and 0.027, 0.029, and 0.057 a.u. with potential V_{II} in th KKR calculations of Faulkner.¹³

C. Superconducting properties

In order to calculate the electron-phonon coupling constant λ and the transition temperature T_c we have also used, besides $m(E_F)$, the angular-momentum—decomposed DOS, $m_l(E_F)$.^{2,3,7} The latter is shown in Table II together with values of the phase shifts and the single-scatterer DOS. η and λ were next calculated according to Eqs. (3) and (4) and the results are shown in Table III. Two sets of results are presented. In the first, (a), the full d - f contribution to η has been considered, while it has been halved for set (b). The latter is necessary since d - f scattering involves electron-ion interaction in the outer portions of the atomic cell where non-muffintin (non-MT) and screening effects, ignored in the rigid MT model being considered here, become important. It has been shown^{3,6} that both these effects significantly reduce the d - f contribution to η , and following Papaconstantopoulos *et al.*,³ we have reduced this contribution by a factor of 2. Next, in

TABLE III. Electronic and superconducting properties of technetium. In set (a) full d - f contribution to η has been considered, while in (b) this has been halved.

	E_F (Ry)	$m(E_F)$ (states/Ry atom spin)	μ^*	η (eV/Å ²)	λ	T_c (K)	
						calc.	expt. ^a
set (a)	0.976	8.275 15	0.13	12.954	0.865 38	15.37	4.6–11.2
set (b)	0.976	8.275 15	0.13	8.9414	0.597 32	5.387	4.6–11.2

^aFrom Ref. 1.

order to calculate T_c , we have set $\mu^* = 0.13$ and used McMillan's expression for the quantity. Dynes²⁸ and Allen and Dynes²⁹ have shown that it is more accurate to use $\omega_{\log}/1.2$ as the prefactor of the exponent in McMillan's equation. This ω_{\log} can be obtained from a Born-von Kármán analysis of neutron scattering data.²⁹ As no such experiment has yet been performed for Tc, we have retained the original McMillan's expression [Eq. (7)] with $\Theta_D = 411$ K.³ It can be seen from Table III that the T_c obtained using the reduced $d-f$ contribution [set (b)] lies within the observed experimental range, but, as is only to be expected from the foregoing discussion and results for other transition elements,³ the T_c obtained considering the full $d-f$ contribution is overestimated. Thus the GG theory,² in spite of the spherical band approximation, appears to have given quite a good idea of the transition temperature of hcp Tc.

D. Optical properties

The electronic energy bands of a crystal have recently acquired primary importance in the study of

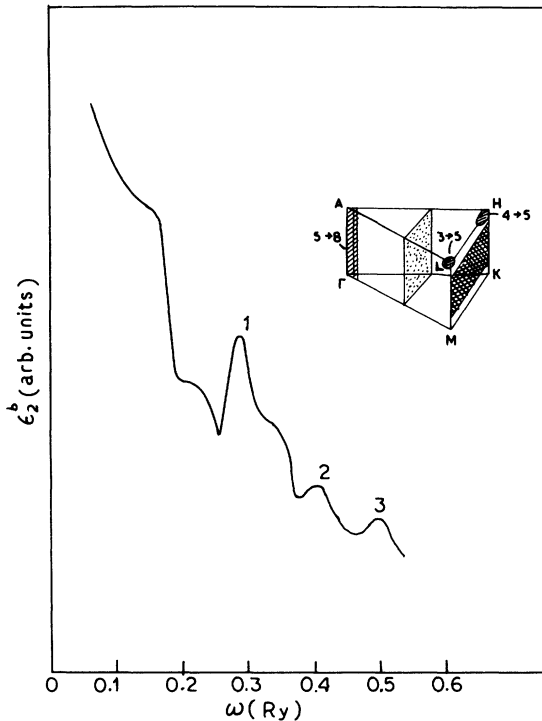


FIG. 4. $\epsilon_2^b(\omega)$ spectrum for Tc. Hatched, crosshatched, and dotted surfaces represent, respectively, the important regions for transitions contributing to peak 1, peaks 1 and 2, and peak 2. The numbers indicate prominent interband transitions. Contributions giving rise to peak 3 are more or less uniformly distributed throughout the BZ.

the optical properties via the imaginary part of the dielectric constant ϵ_2^b in light of recent experiments by Weaver *et al.*¹² In order to calculate ϵ_2^b , the irreducible $\frac{1}{24}$ th wedge of the BZ was divided into 126 microhexagons and the energy in each microzone was calculated from first principles. The JDOS, proportional to $\omega^2 \epsilon_2^b$, was then obtained by the stabilized histogram method. It would have been more accurate^{11,22} to have considered a finer mesh of points and used the Raubenheimer-Gilat method which incorporates a first-order fit to the energy surfaces instead of the zeroth-order fit as in the histogram scheme. However, as no calculation of the optical properties of Tc either experimental or theoretical exists to date, we feel that even this somewhat crude approach would be rather useful as it has the demonstrated^{25,30,31} potentiality of bringing out the salient features of the $\epsilon_2^b(\omega)$ spectrum.

The ϵ_2^b histogram thus calculated stabilizes at $\Delta\omega = 0.03$ Ry and is shown in Fig. 4. There are three peaks in the curve centered at 0.285, 0.405, and 0.495 Ry with the first being the most prominent. A shoulder is also seen just beyond the first peak. The inset to the figure identifies the bands chiefly responsible for, and the location in \vec{k} space where, the important transitions contributing to peaks labeled 1 and 2 occur. The transitions giving rise to the high-energy peak marked 3, however, are uniformly distributed throughout the BZ.

V. CONCLUSIONS

In this paper we have presented detailed calculations of the energy-band structure of Tc and tried to predict the density of states, the Fermi surface, and the superconducting properties and the imaginary part of the dielectric function from this data. In particular, the calculations of the electron-phonon coupling constant and the superconducting transition temperature have been rigorously performed in accordance with the theory of Gaspari and Gyorffy without resorting to any arbitrary assumptions with respect to structure or otherwise as has been done by previous workers^{3,5} in this field. Therefore, the rather good experimental agreement obtained for the transition temperature, and to a lesser extent of the Fermi surface, is a measure not only of the accuracy of the APW method but also of the potentials computed via the $X\alpha$ exchange approximation. The present calculations also constitute the first effort to predict the optical properties of Tc.

Finally, we would like to point out that the one remaining weakness of the present calculations is that they are non-self-consistent (NSC). However,

the NSC APW calculations of Mattheiss³² (using the $\alpha=1$ exchange) for Nb, which lie close to Tc in the Periodic Table, have shown generally very good agreement with experimental results. Although the exchange used in this paper is $X\alpha$, the fact that the properties predicted in this paper agree more or less satisfactorily with experiments, wherever these are available, indicates that the present calculations would add to the understanding of the band structure and properties of Tc in light of the paucity of

data for this metal as compared to its neighbors in the Periodic Table.

ACKNOWLEDGMENTS

The author is grateful to Professor A. K. Barua and to Dr. A. K. Batabyal for their keen interest in the subject. She is also thankful to the Council for Scientific and Industrial Research, New Delhi, for financial assistance during the course of this work.

-
- ¹B. W. Roberts, *J. Phys. Chem. Ref. Data* **5**, 724 (1976).
²G. D. Gaspari and B. L. Gyorffy, *Phys. Rev. Lett.* **28**, 801 (1972).
³D. A. Papaconstantopoulos, L. L. Boyer, B. M. Klein, A. R. Williams, V. L. Moruzzi, and J. F. Janak, *Phys. Rev. B* **15**, 4221 (1977).
⁴W. L. McMillan, *Phys. Rev.* **167**, 331 (1968).
⁵R. Asokamani and K. Iyakutti, *J. Phys. F* **10**, 1157 (1980).
⁶L. L. Boyer, B. M. Klein, and D. A. Papaconstantopoulos, *Ferroelectrics* **16**, 291 (1977).
⁷D. A. Papaconstantopoulos and B. M. Klein, *Phys. Rev. Lett.* **35**, 110 (1975).
⁸B. M. Klein, D. A. Papaconstantopoulos, and L. L. Boyer, in *Proceedings of the Second Rochester Conference on Superconductivity in d- and f-band Metals, Rochester, New York, 1976*, edited by D. H. Douglass (Plenum, New York, 1976) p. 339.
⁹P. Chatterjee, *Phys. Status Solidi B* **97**, 273 (1980).
¹⁰P. Chatterjee, *Can. J. Phys.* **58**, 1383 (1980).
¹¹W. E. Pickett and P. B. Allen, *Phys. Rev. B* **11**, 3599 (1975).
¹²J. H. Weaver, D. W. Lynch, and C. G. Olson, *Phys. Rev. B* **7**, 4311 (1973); **10**, 501 (1974).
¹³J. S. Faulkner, *Phys. Rev. B* **16**, 736 (1977).
¹⁴A. J. Arko, G. W. Crabtree, S. P. Hörnfeldt, J. B. Ketterson, G. Kostorz, and L. R. Windmiller, in *Low Temperature Physics—LT 13*, edited by K. D. Timmerhaus, W. Josullivan, and E. F. Hammel (Plenum, New York, 1974), Vol. 4, p. 104.
¹⁵H. Schlosser and P. M. Marcus, *Phys. Rev.* **131**, 2529 (1963).
¹⁶T. L. Loucks, *Augmented Plane Wave Method* (Benjamin, New York, 1967), p. 47.
¹⁷F. Herman and S. Skillman, *Atomic Structure Calculations* (Prentice-Hall, Englewood Cliffs, 1963).
¹⁸K. Schwarz, *Theor. Chim. Acta* **34**, 225 (1974).
¹⁹C. J. Smithells, *Metals Reference Book*, 5th ed. (Butterworths, London, 1976), p. 118.
²⁰L. F. Mattheiss, J. H. Wood, and A. C. Switendick, *Methods in Computational Physics* (Academic, New York, 1968), Vol. 8, p. 142.
²¹L. J. Raubenheimer and G. Gilat, *Phys. Rev.* **157**, 586 (1967).
²²J. F. Janak, in *Computational Methods in Band Theory*, edited by P. M. Marcus, J. F. Janak, and A. R. Williams (Plenum, New York, 1971), p. 323.
²³W. John, *J. Phys. F* **3**, L231 (1973).
²⁴B. L. Gyorffy, in *Proceedings of the Second Rochester Conference on Superconductivity in d- and f-band Metals, Rochester, New York, 1976*, Ref. 8, p. 29.
²⁵M. Sen and S. Chatterjee, *J. Phys. F* **10**, 985 (1980).
²⁶R. Asokamani, K. Iyakutti, and V. Devanathan, *Solid State Commun.* **30**, 385 (1979).
²⁷L. F. Mattheiss, *Phys. Rev.* **151**, 450 (1966).
²⁸R. C. Dynes, *Solid State Commun.* **10**, 615 (1972).
²⁹P. B. Allen and R. C. Dynes, *Phys. Rev. B* **12**, 905 (1975).
³⁰J. Chowdhuri, P. Chatterjee, and S. Chatterjee, *J. Phys. F* **9**, 683 (1979).
³¹P. M. Holtham, J. P. Jan, and H. L. Skriver, *J. Phys. F* **7**, 635 (1977).
³²L. F. Mattheiss, *Phys. Rev. B* **1**, 373 (1970).